Automotive and Engine Technology (2023) 8:177–192
https://doi.org/10.1007/s41104-023-00132-0

ORIGINAL PAPER

An experimental study on aging effects of the air–fuel ratio swing on modern gasoline three-way catalysts

René Eickenhorst[1,2] · Thomas Koch[1]

Received: 5 February 2023 / Accepted: 30 June 2023 / Published online: 20 July 2023

Abstract
Today's governmental legislations require region specific emission standards for passenger vehicles. Continuously increasing legal requirements demand the development of more complex exhaust gas after treatment systems to further reduce harmful gases like carbon monoxide (CO), hydrocarbons (HC) and nitrogen oxides (NO_x). Due to specific load profiles and other boundary conditions, the efficiency of the aftertreatment system declines over lifecycle, so that the emissions might increase. Consequently, the durability of the system becomes a critical design parameter with upcoming legislation demanding emissions stability over the vehicle life cycle. Within this publication, catalyst aging effects due to air–fuel ratio (AFR) swing are analyzed experimentally. To create catalyst aging conditions, a modern eight-cylinder turbocharged engine was modified and specific aging cycles with a variation of AFR swing amplitude and frequency were conducted. Light-off curves were used to depict the negative impact of the AFR swing on the aging catalyst systems. A higher swing frequency resulted in an increased temperature amplitude within the entrance area of the catalyst, while an elevated amplitude lead to more exothermic heat release and stronger aging over the complete catalyst, as visualized via conversion maps. A theoretical calculation of thermal loads by Arrhenius equation supports the results and indicates the direction of supplementary experimental approaches.

Keywords Catalyst aging/deactivation · Upcoming emissions legislations · Vehicle durability · Air–fuel ratio swing · Light-off · Conversion efficiency maps · Oxygen storage capacity · Exothermic behavior · Arrhenius equation

Abbreviations

AFR	Air–fuel ratio
BEV	Battery electric vehicle
Ce	Cerium
cGPF	Coated gasoline particular filter
CO	Carbon monoxide
ECU	Engine control unit
GPF	Gasoline particular filter
HC	Hydrocarbon
HEV	Hybrid electric vehicle
ICE	Internal combustion engine
LO	Light-off
NO_x	Nitrogen oxide
O_2	Oxygen
OBD	On-board diagnosis
OSC	Oxygen storage capacity
Pd	Palladium
PGM	Platinum group metals
Pt	Platinum
PHEV	Plug in hybrid electric vehicle
Rh	Rhodium
SA	Secondary air
SAI	Secondary air injection
SRC	Standard road cycle
TWC	Three-way catalyst
T_{90}	Sensor response time

✉ René Eickenhorst
rene.eickenhorst@mercedes-benz.com

Thomas Koch
thomas.a.koch@kit.edu

[1] IFKM (Institut für Kolbenmaschinen), KIT, Karlsruhe, Germany

[2] Mercedes-AMG GmbH, Affalterbach, Germany

1 Introduction

Individual traffic is a growing demand within global population. Due to the resulting increase of air pollution, public awareness concerning environmental impacts have increased. Public demand for preservation of air quality lead governments to implement stricter country-specific

legislation for exhaust emissions. Besides the further reduction of threshold value for already limited emissions, regulations concerning the durability and emission stability of aftertreatment systems were introduced. Current EU6d type V legislation demands service life for the exhaust gas aftertreatment of passenger cars up to 160,000 km, with current prediction of the EU7 legislation proposing an additional extension of around 25% [1]. To fulfill these requirements, a trend towards electrification of vehicle powertrains started a couple of years ago. Besides battery electric vehicles (BEV) and hybrid-systems (HEV & PHEV), conventional powertrains with an ICE (internal combustion engine) will be needed as vehicle powertrain for the next years. Therefore, it is important to optimize its technology to ensure the compliance with upcoming requirements. One of the major components for gas aftertreatment of a gasoline engine is the three-way catalyst (TWC), responsible for the reduction of harmful exhaust gases like carbon monoxide (CO), hydrocarbons (HC) and nitrogen oxide (NO_x) during engine operation. To accomplish low emissions, a stoichiometric equilibrium of oxidation and reduction processes in the TWC is required. Due to driver-specific load requirements and system response lag, this specific air–fuel ratio (AFR) cannot be provided in all engine operation modes. An AFR swing around the stoichiometric operation mode is used for storage of excessive oxygen during lean phases within the catalysts, providing oxidative species during rich phases. Within this article, the influence of the air–fuel ratio on the catalyst durability is analyzed under high load conditions and different AFR swing characteristics.

2 Catalytic deactivation (state of the art)

2.1 Exhaust gas aftertreatment of a gasoline combustion engine

The exhaust gases of gasoline engines contain pollutants resulting from incomplete combustion of gasoline/air mixture. Specific emission standards, which are partly harmonized by regional legislation, regulate the individual amount of harmful substances generated by gasoline powered vehicles. Upcoming legislation with reduced limits will demand vehicle manufactures to develop more effective exhaust gas aftertreatment technologies to fulfill these requirements. Table 1 provides an overview of the development of European regulation of harmful gases for gasoline passenger cars and its limits (Fig. 1).

Modern state of the art exhaust gas aftertreatment systems consist of one or more catalytic converters as well as

Table 1 Reduction of threshold values for gaseous emissions of passenger cars [2, 3]

Legislation	Year	Gas emissions					Particle emissions	
		CO (mg/km)	THC (mg/km)	NMHC (mg/km)	NO_x (mg/km)	NH_3 (mg/km)	PM (mg)	PN (–)
EURO 3	01/2000	2300	200	–	150	–	–	–
EURO 4	01/2005	1000	100	–	80	–	–	–
EURO 5	09/2009	1000	100	68	60	–	4.5	–
EURO 6	09/2014	1000	100	68	60	–	4.5	6.0×10^{11}
EURO 7	07/2025	500	100	68	60	20	4,5	6.0×10^{11}

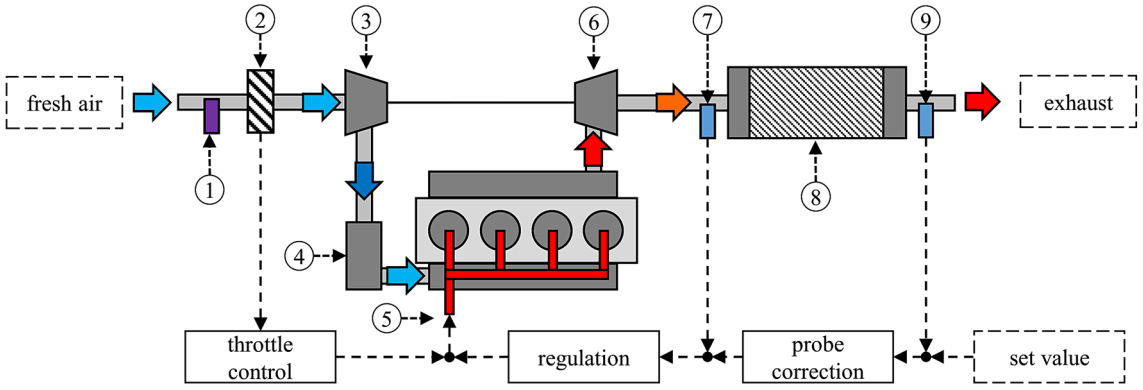

Fig. 1 Simplified diagram of the air–fuel control of a turbocharged four-cylinder engine (according to Riegel et al. [4]); (1) airflow sensor; (2) throttle; (3) compressor; (4) charge-air intercooler; (5) fuel system; (6) turbocharger; (7 and 9) oxygen sensor; (8) three way catalyst (TWC)

a complex air–fuel management system. The catalytic converters use finely dispersed precious metal coating (PGM) to reduce the harmful tail pipe emissions via chemical conversion by reducing NO_x and oxidizing CO and HC emissions at the same time. The optimum for the reduction of these harmful gases is specified around a stoichiometric AFR. For average gasoline, the value is set around 14.7. The relation between the current and the stoichiometric AFR is named λ, illustrated in Fig. 2 [5]:

$$\text{Stoichiometric AFR} = \frac{m_{\text{air}}}{m_{\text{fuel}}} = 14.7 \quad \text{Air fuel ratio (AFR)}, \tag{1}$$

$$\lambda = \frac{\text{current AFR}}{\text{stoichiometric AFR}} = \frac{\frac{m_{\text{air}}}{m_{\text{fuel}}}}{14.7} \quad \lambda. \tag{2}$$

AFR is measured by oxygen sensors in the aftertreatment system [7]. By changing injection quantity as well as throttle position, this ratio can be adapted. Figure 1 shows a simplified structure of the AFR control of a turbocharged four-cylinder engine.

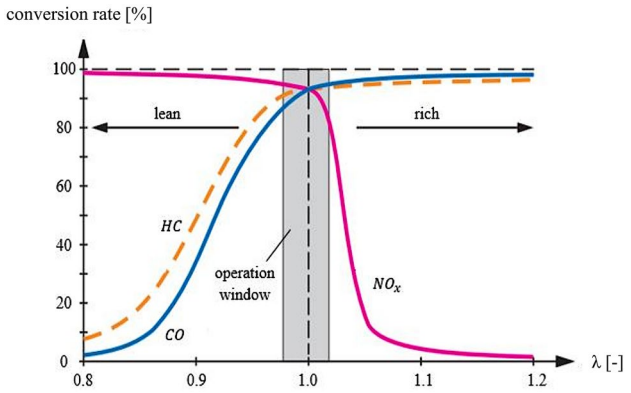

Fig. 2 Conversion rate over λ of a gasoline engine [6]

2.2 Three-way catalyst

The TWC is one of the main components of the exhaust gas aftertreatment system of a gasoline engine. The chemical conversion can be separated into oxidative and reductive reactions. Both reactions can take place at the same time during a stoichiometric engine operation point ($\lambda \approx 1$).

$$2CO + O_2 \rightarrow 2CO_2 \quad \text{Oxidation I}, \tag{3}$$

$$4C_xH_y + (4x + y)O_2 \rightarrow 4x\,CO_2 + 2y\,H_2O \quad \text{Oxidation II}, \tag{4}$$

$$2NO + 2CO \rightarrow N_2 + 2CO_2 \quad \text{Reduction}. \tag{5}$$

Although these reactions are exothermic, an activation energy relating to PGM surface temperatures of around 200–300 °C is required to start the process. To provide these thermal conditions, in modern exhaust systems the TWC is located as close as possible to the exhaust valve. By shortening the exhaust path, thermal inertia losses and light-off time are reduced maximizing the conversion rate of raw to tailpipe. Due to high exhaust mass flow of modern combustion engines, sufficient active catalytic surface has to be provided to ensure the complete conversion at any load. State of the art TWCs (Fig. 3) consist of ceramic materials to fulfill high demands regarding thermomechanical stability and pressure loss. The ceramic monolith (substrate), embedded in a canning, provides a maximized surface area at given volume. It consists of honeycombed channels with a washcoat, mainly consisting of Al_2O_3 to increase the channel surface by a factor of about 7000 [6]. The ability to store and release oxygen under specific conditions is realized by addition of cerium

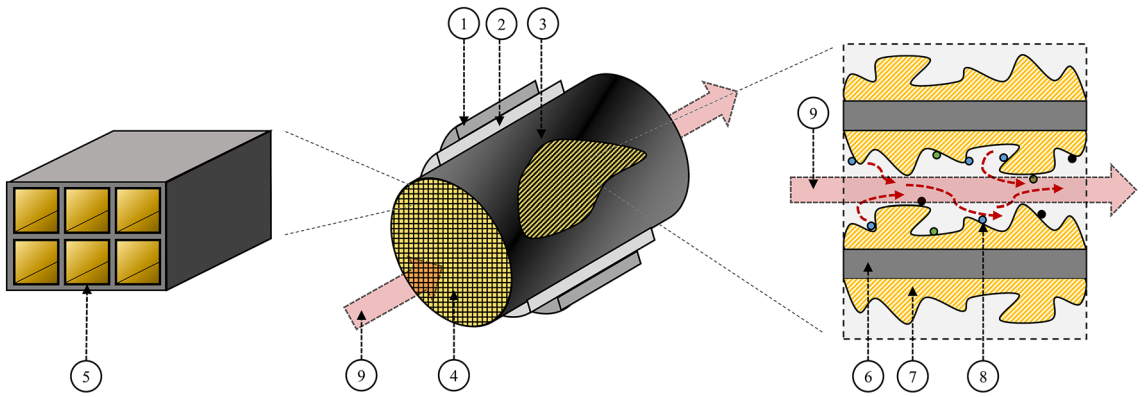

Fig. 3 Schematic setup of a modern ceramic three-way catalyst; (1) canning; (2) damping mat; (3) ceramic monolith; (4) front surface; (5) channels; (6) ceramic wall; (7) washcoat; (8) fine-distributed precious metals; (9) exhaust gas flow direction

dioxide (CeO_2). On top of this washcoat, finely dispersed precious metal particles like rhodium (Rh), palladium (Pd) and platinum (Pt) are employed to provide the desired catalytic activity. As a result of rising platinum prices, the use of Pd-Rh catalysts is increasing [5, 7–10].

2.3 Oscillating air–fuel ratio (AFR) swing

Stoichiometric operation is a key parameter to reduce tailpipe emissions to a minimum. Due to system response lag (exhaust gas flow and sensor delay), modern systems are calibrated to oscillate the AFR around the stoichiometric value [11]. The so-called AFR-swing in combination with temporary oxygen storage enables oxidation and reduction processes to take place at the same time. Excessive oxygen is stored by cerium oxides within the washcoat during lean phases and is provided to precious metals during the rich phases. A higher oxygen storage capability of the catalyst permits the use of a more intense AFR-swing [7].

2.4 Deactivation methods of a modern three-way catalyst

The catalytic activity of a three-way catalyst declines under certain operating conditions over the life cycle of a passenger car. Loss of effectiveness due to a reduction of conversion rate is the consequence. As a result, the pollutant emissions of the car may rise over its life cycle, although emissions still have to fulfill the legal standards at the requested mileage. Catalyst aging can be generally separated into four different mechanisms: chemical poisoning, fouling, mechanical abrasion and thermal sintering [7], listed in Table 2.

During deactivation by chemical poisoning, active elements like sulfur and lead are blocking the catalytic centers by reacting with the precious metals like Platinum (Pt) and Rhodium (Rh). Deactivation by sulfur on Pt–Rh catalyst is found to be partially reversible. In most cases it is not, especially for catalysts with a combination of Pd and Rh and monoliths made out of CeO_x and Al_2O_3 [12, 13]. Due to the low amount of lead and sulfur in modern gasoline fuel standards, chemical poisoning plays only a minor role today. Fouling describes the geometrical blockage of the catalysts surface resulting in less active surface area being able to take part in chemical reactions, often caused by deposits. Mechanical collapse or functional failure of the substrate and its washcoat by previous high temperature stress is referred to as mechanical aging. Due to the loss of surface area, reduction and oxidation processes are decreased due to reduced precious metals and deteriorating oxygen storage capacity [14]. Additionally, mechanical abrasion can occur by particles formed during combustion processes or stripping deposits of the engine periphery flowing through the catalyst itself. Another mechanical degradation mechanism are resulting of thermal shocks by extreme temperature gradients on the substrate surface exceeding 15 K/ms, caused for instance by misfire. The high temperature gradients overstress the substrate mechanical stability, causing chipping of material layers [15]. Thermal sintering is stated to be the most important factor regarding deactivation of modern catalysts. Due to its high significance and the possibility to use thermal load as a controlled parameter for synthetic aging, the process of sintering and its consequences are described in the following chapter in detail.

2.5 Thermal sintering as a main function for catalyst deactivation

Due to rising legal requirements and challenging emission test cycles with lower emission thresholds and higher engine load requests, the reduction of cold start phase duration is one of the central factors to minimize exhaust emissions. In most current exhaust system setups, the first catalytic converter is positioned as close as possible to the outlet valve of the combustion engine. This results in a reduction of heat losses and an improvement of the light-off behavior of the catalytic converter [16]. To ensure faster catalyst heat up, the average applied operating temperature during the vehicle life cycle is set on an elevated higher plateau, which might increase aging and therefore emission long-term stability.

Thermal aging in general is a slow, gradual process as a function of temperature and time [17]. Depending on the washcoat's mix of materials as well as types and amount of precious metals, the aging behavior can be different [7]. As an example, a combination of palladium or platinum interact in a different way when combined with rhodium [18]. With higher operating temperature, a more aggressive aging via sintering processes can be observed. Therefore, critical temperatures above a component-specific thermal limit have to be avoided. First sintering degradations are documented between temperatures of 800–900 °C, whereas

Table 2 Main mechanism of catalyst deactivation [7]

Chemical	Fouling	Mechanical	Thermal sintering
Reduction of catalytic activity by blocking surface of precious metals	Reduction of surface by blocking overall surface	Degradation due to abrasion and thermal shock of the monolith (front surface)	Substrate and washcoat collapse due to high temperatures

maximum exhaust temperature operation points can reach around 1000 °C [17]. At these temperatures, the fine and evenly distributed precious metal particles start to agglomerate by both atomic and crystalline migration processes [6, 7], resulting in an increase of single particle volume and a drastic reduction of overall active catalytic surface area [18]. This process will even be intensified by the presence of oxidative atmosphere [19]. Temperatures above the thermal limit may further induce alloy phase changes within the washcoat, so that a surface collapse of over 95% could be observed [7]. This collapse embeds the catalytic centers within the washcoat, so these are not able to take part in reactions furthermore (Fig. 4). High emissions during normal vehicle operation due to strongly reduced catalytic activity are the consequences.

3 Experimental methods

3.1 Experimental setup

The following chapter provides information regarding the experimental setup. It describes the engine test bench and its modification used for implementing the catalyst aging procedure. Furthermore, the catalytic exhaust system and its sensor system for regulating the AFR swing under required boundary conditions are specified. Additionally, an overview regarding the design of experiments as well as a possible evaluation regarding the identification of the influence of the AFR swing on the catalyst aging are provided.

3.1.1 Catalytic exhaust system of a modern four cylinder engine and its sensor systems for the synthetic engine bench aging process

An aftertreatment system of the current four-cylinder engine of Mercedes-AMG GmbH has been selected for the experiments. The system with its layout, washcoat and layer technology is state of the art and consists of a one-bank system, therefore allowing parallel aging of two exhaust systems on a single V-engine test bench to reduce the costs as well as simplifying the handling within the test facilities. As in most modern systems, the hotend contains two different substrates: a TWC at the front and a gasoline particular filter (GPF) at the back. The GPF is equipped with a reactive coating (cGPF) supporting catalytic conversions as well. Both substrates share an overall catalytic volume of 3.701 L (TWC = 1.558 L; cGPF = 2.143 L). The synthetic engine bench aging process is controlled via thermocouples installed upstream, within and downstream the TWC, as well as downstream the cGPF. Due to the high exhaust gas temperature close to 1000 °C, sensors of the type K have been chosen. Oxygen sensors, installed up- and downstream of the TWC, are utilized to regulate the AFR and the OSC determination. For calculation of the TWC's and GPF's emission conversion ratio and the corresponding overall performance of the system, sampling points for raw gas emissions are set up in front of the TWC and GPF, allowing the measurement of CO, NO_x and HC-emission.

3.1.2 Modification of turbocharged engine for catalyst aging on an engine test bench

Synthetic catalyst aging on an engine test bench is cost-efficient, takes less time due to well-controlled engine operation with a highly repeatable accuracy and results much more compared to reality-aged catalysts via vehicle mileage accumulation [20]. The test bench aging is usually performed via a natural aspirated engine. This type of engine has the advantage of providing high exhaust gas temperatures above 950 °C behind the exhaust manifold, respectively in front of the TWC, without violation of any component temperature durability limits. For the present study, catalyst aging requires high exhaust temperatures, a defined adjustable AFR as well as a specific controllable high exhaust mass flow at lower engine speed, which can only be provided by a turbocharged engine. To compensate the enthalpy losses due to the turbocharger components in order to reach high catalyst temperatures, the temperature level behind the outlet valve (T3 temperature) needs to be elevated, exceeding

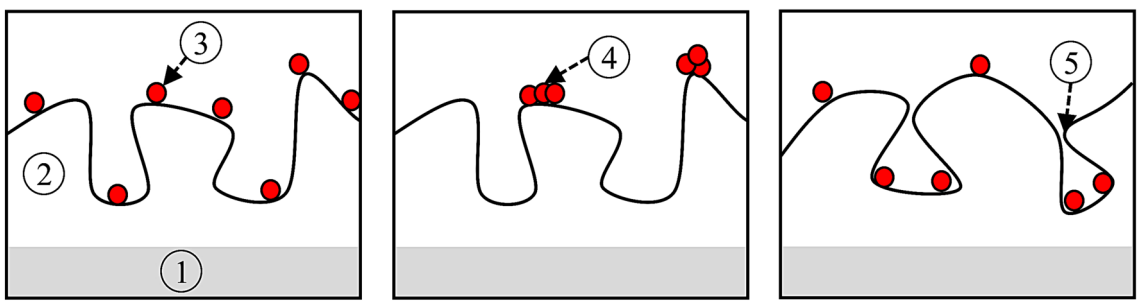

Fig. 4 Sintering process of washcoat (2) on a monolith (1) and active catalytic material (3); agglomeration (4) and embedding (5)

the given temperature durability limit of the turbocharger components. Therefore, modifications are required for preventing a part failure during long catalyst aging processes. The main part of the modification consists of the integration of a secondary air injection into the exhaust control path behind the turbocharger of each bank. By using an overall rich combustion and a downstream injection of fresh air, the temperature within the catalysts rises due to exothermic reaction of HC with the precious metals. The catalysts temperature and exhaust AFR are adjusted by regulation of the engine AFR as well as the secondary air mass flow ratio. To guarantee a fixed AFR in front of the catalyst, the exhaust gas and the secondary air are homogenized by a mixer, installed upstream of the catalyst. Additional experiments have been performed to ensure homogeneous gas composition. Figure 5 displays the hardware modification of the turbocharged V8 engine used for bank-individual thermal catalyst aging. By providing rich engine exhaust gas, the temperature of the turbocharge components (3 in Fig. 5) are within the parts thermal specifications.

3.2 Design of experiment

3.2.1 Experimental procedure

The catalyst AFR can be regulated in two different ways by the described setup: either by using a constant engine AFR and a variation of the mass flow of the SA injection, or vice versa. Due to the slower response time of the SA system, the engine AFR was regulated via the fuel injection resulting in an oscillating swing to rich conditions for the presented experiments. The constant SA flow increases the overall AFR, so that a sinusoidal swing around the stoichiometric operation is achieved. During normal driving conditions, the frequency of this AFR swing is around one to two Hertz. This small frequency ensures continuous oxidation and reduction on the catalyst surface while maintaining an overall stoichiometric operation, measured with the secondary oxygen sensor downstream the first catalyst. By reducing the frequency, the catalyst is not able to buffer the amount of oscillating rich or lean exhaust gases, so probe voltage of the secondary oxygen sensor starts to fluctuate as well. Figure 6 displays the influence of AFR frequency: with lower frequency, higher ranges of alternating lean and rich phase can be observed within the catalyst.

To determine the aging effect of AFR swing on the complete catalyst surface, AFR frequency is set up to the lowest value at which the voltage of the secondary oxygen sensor starts to fluctuate as well. Response time (T_{90}) of the oxygen sensors is set up as a characteristic curve within the ECU, so that the response of the sensor has already been compensated for. Figure 7 shows the constant secondary air- and the swinging engine exhaust mass flow, resulting in an AFR swing in front, as measured with the upstream oxygen sensor, and over the complete catalyst, displayed by a fluctuating voltage of the secondary oxygen sensor. The secondary oxygen sensor used within this study shows a stoichiometric AFR with a value about 700 mV.

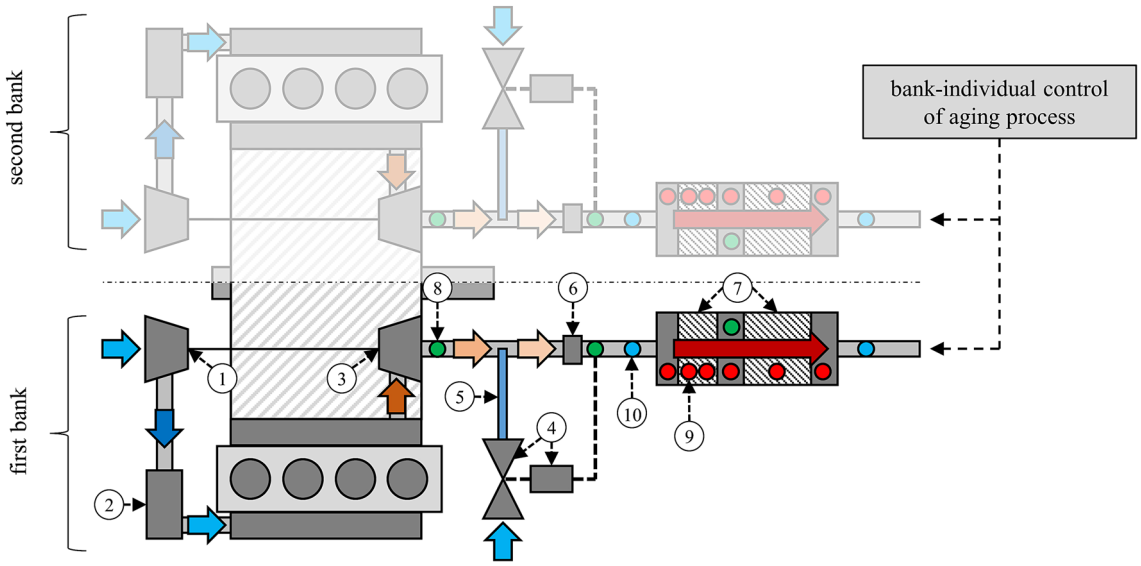

Fig. 5 Modification of the turbocharged V8 engine – only one bank is illustrated, (1) compressor; (2) charged air cooler; (3) turbo charger; (4) secondary air regulation system and valve; (5) secondary air injection; (6) mixer; (7) monoliths; (8) oxygen sensor; (9) thermocouples; (10) gas extraction point

3.2.2 Frequency and amplitude of the air–fuel ratio swing

Five identical exhaust systems have been synthetically aged on engine test bench with a swing variation of AFR. During the aging process, the engine operating point has been held constant to exclude further influences on the catalyst aging provoked by engine load changes. To clearly identify the aging influence of the swing, the first exhaust system was aged without any sinusoidal swing at a stoichiometric ratio, fluctuating between 0.99 and 1.005. The second system was aged with a frequency of air–fuel ratio of 0.25 Hz with an amplitude of 0.063. This defines a periodic cycle of 4 s and a swing amplitude from 0.937 to 1.063. For third and forth test, the amplitude, respectively the frequency has been changed as stated in Table 3.

3.2.3 Aging boundary conditions

Measurements of fresh exhaust systems indicated production deviations based on the manufacturing and coating process of the layer resulting in different light-off and OSC behavior as an identical mixture and allocation of the precious metal particles cannot be guaranteed. To ensure that the aging results are independent from these deviations, all exhaust systems were subjected to a conditioning pre-sintering process on the engine test bench. A pre-sintering during a short time of around 3 h under medium aging temperature of 850 °C leveled the agglomeration and embedding of the fine dispersed catalytic precious metals, ensuring a comparable light-off and OSC behavior.

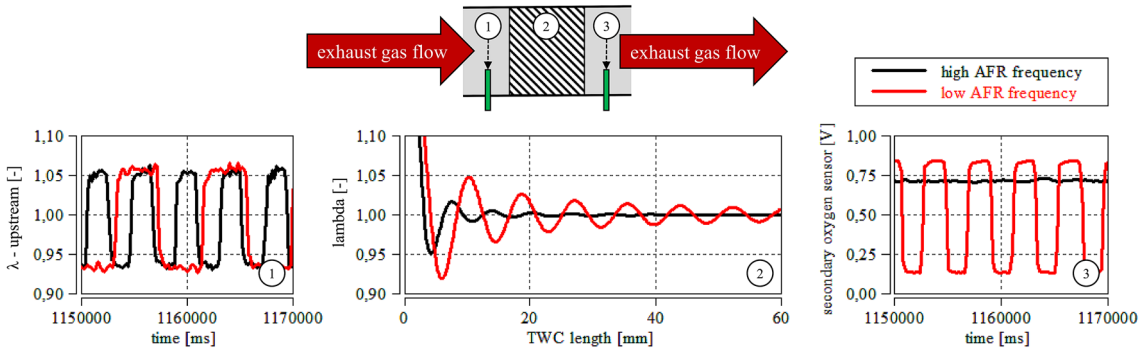

Fig. 6 Range of the alternating lean and rich phase within the TWC (2) depending on its frequency, measured with the first (1) and secondary oxygen sensor (3)

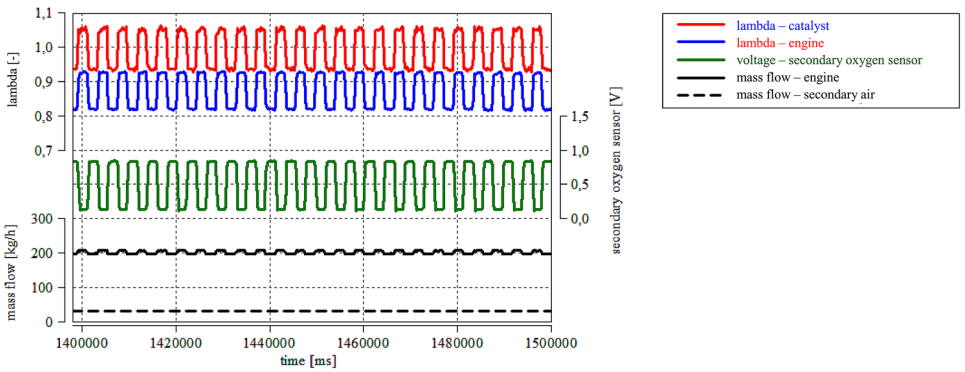

Fig. 7 Rich engine λ with a constant secondary air injection to ensure an overall AFR swing within the catalyst around the stoichiometric working point, measured via secondary oxygen sensor after the catalyst

Table 3 AFR swing variation—design of experiments

Test	Exhaust system ID	Catalyst temperature (°C)	Catalyst mass flow (kg/h)	AFR frequency (Hz)	AFR amplitude (–)	Description
#1	#486	≈ 950	≈ 200	≈ 0	≈ 0	Constant AFR (no swing)
#2	#487			0.25	0.063	Baseline AFR swing
#3	#488			0.125	0.063	Low AFR swing frequency
#4	#490			0.25	0.08	High AFR swing amplitude

Overall exhaust mass flow within the catalyst has been defined as the sum of the engine exhaust mass flow and the mass flow of the injected secondary air. The experimental setup allowed an overall mass flow exceeding the desired target values. To focus on an AFR swing representative for a vehicle operating point, the exhaust mass flow was regulated at around 200 kg/h. 1.5 mm thermocouples, installed within the catalyst, were used to monitor gas temperature including the exothermic effects. Due to the high thermal inertia of the second temperature sensor within the catalyst, engine control was based on the first thermocouple. To reduce time and cost of the catalyst aging, the temperature had to be set as high as possible within the allowed boundary conditions to shorten bench time. Based on previous aging experiences with this type of catalyst, the aging temperature was set to $950 \pm X$ °C for 50 h to ensure an aging effect generated by different AFR swings.

Figure 8 illustrates four different sets of AFR frequencies and amplitudes as listed in Table 3, resulting in different temperature profiles over time, measured with a 1.5 mm type K thermocouple at one-third TWC length after the front surface. The failure tolerance of this type of sensor at temperatures of around 950 °C is stated as ± 3.8 K. As shown in Fig. 8 at the aging process of catalyst #486, the process control exhibits a temperature oscillation around 950 °C of about ± 2.5 K. In addition to this, the temperature influence in range of the sensor tolerance value on the catalyst aging progress is marginal, so that tolerances of the thermocouples can be neglected.

3.3 *Determination of catalyst aging grade* via *oxygen storage capacity and light-off behavior*

Legal regulations demands a health monitoring for the catalytic system. As deactivation like sintering also affects the washcoat, the amount of storable oxygen can be used for the determination of the degree of aging of an exhaust gas aftertreatment system via a special on-board diagnosis (OBD), triggered by the engine control unit (ECU). During specific driving maneuvers, the maximally stored oxygen mass can be determined with the following formula [5]. m_{O_2} defines the oxygen storage capacity, t_0 and t_1 correspond to

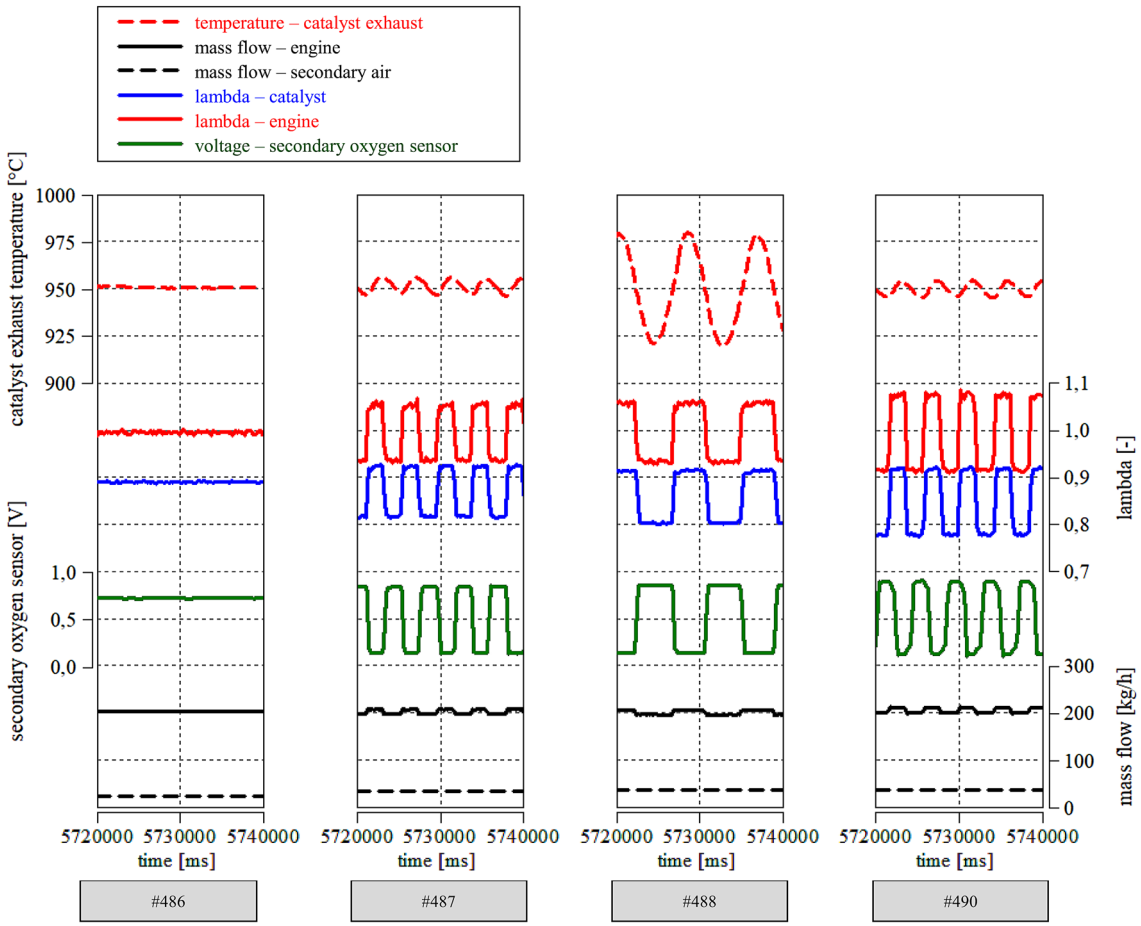

Fig. 8 λ parameters: test #486 to #490 from left to right with the exhaust systems listed in Table 3

the duration of the triggered lean to rich switches as recognized by the oxygen sensor in the front and in the back of the catalyst. The amount of oxygen, which can be stored within the catalyst, depends on a variation of influence factors and cannot be generalized [5, 21]:

$$m_{O_2} = \int_{t_0}^{t_1} 0.23\left(\lambda_{\text{engine}}(t) - 1\right)\, \dot{m}_{\text{air}}(t)\, \mathrm{d}t \quad \text{Oxygen storage capacity.} \tag{6}$$

The m_{O_2} value is then compared with a characteristic diagram of new catalysts and stored within the ECU to define the health status. The more oxygen storage capacity a catalyst can provide, the more oxidative processes are possible during rich conditions. The following formulas describe the chemical reaction of injection and dissipation of oxygen in cerium oxides [6, 10]:

$$2Ce_2O_3 + O_2 \rightarrow 4CeO_2 \quad \text{Oxygen injection,} \tag{7}$$

$$2CeO_2 + CO \rightarrow CeO_3 + CO_2 \quad \text{Oxygen dissipation I,} \tag{8}$$

$$2\left(2y + \frac{1}{2}z\right)CeO_2 + C_xH_y \rightarrow \left(2y + \frac{1}{2}z\right)Ce_2O_3 + yCO_2 + \frac{1}{2}zH_2O \quad \text{Oxygen dissipation II.} \tag{9}$$

Cerium(IV)oxide (CeO_2) is the most important ingredient for raising the OSC within the washcoat with Rhodium(IV) oxide (RhO_2) supporting this ability as well [7, 11]. The transferable mass of oxygen, called oxygen storage capacity (OSC), depends on temperature and mass flow [7, 17, 22]. As described before, the catalytic activity also depends on the catalyst temperature itself. The efficiency of conversion can be given as a function of temperature in Fig. 9 with higher temperature allowing for increased conversion rates. At temperatures below 100 °C, no conversion be observed. While temperatures increase up to around 300 °C, catalytic reactions are controlled mainly by reaction kinetics. Within this phase, heat is transmitted to the catalyst from the exhaust gas. After reaching the light-off temperature, or so-called ignition, the catalyst creates heat due to its exothermic reactions [23]. With further rising temperatures, conversion limitation is determined by pore diffusion inside the washcoat. As described in chapter 7.2, the substrate provides a large surface area with a small pore size, so that the mass transport between the exhaust gas and the PGM is limited by temperature-dependent pore diffusion. At high temperatures, the bulk mass transfer of all reactants taking part in the conversion occurs between the gas phase and the washcoat [11]. The T_{50}-temperature, defined as catalyst temperature at which 50% of raw gas emissions are converted, is a commonly constant to describe the aging progress of a catalyst. With increasing catalyst deactivation, more thermal energy has to be provided to reach ignition, resulting in reaction curves, shifted to higher temperatures with a higher T_{50} [17].

3.4 Calculation of conversion maps

The light-off behavior of an exhaust system component describes the catalytic activity for each gaseous emission as a function of conversion rate of raw gas emissions over the catalyst temperature. As a consequence of a variable exhaust mass flow during cold starts, provoked by driver-specific load requirements, exhaust temperature is transient. To consider this dependency, the conversion rate is provided as a function of exhaust mass flow and catalyst temperature by a heat map diagram, calculated by the workflow illustrated in Fig. 10.

The conversion rate of each raw gas emissions component was determined on the engine test bench at different constant engine load points with different exhaust mass flow values. By controlling the engine load and corresponding exhaust mass flow, influences on the catalyst temperature

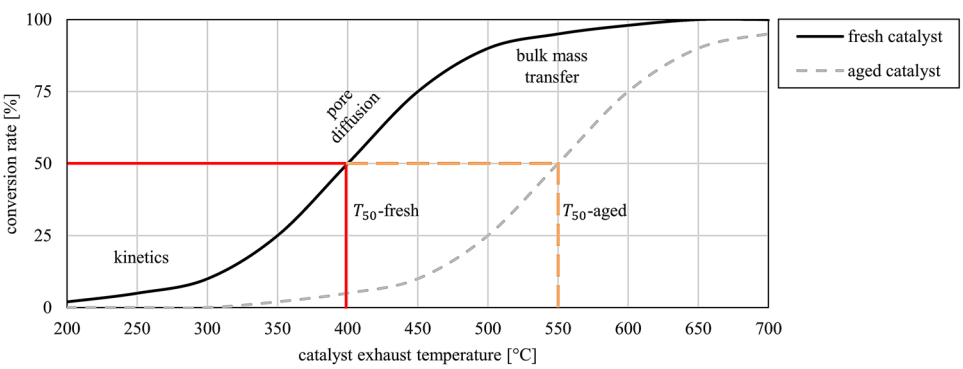

Fig. 9 Schematic catalyst light-off behavior depending on catalyst exhaust temperature

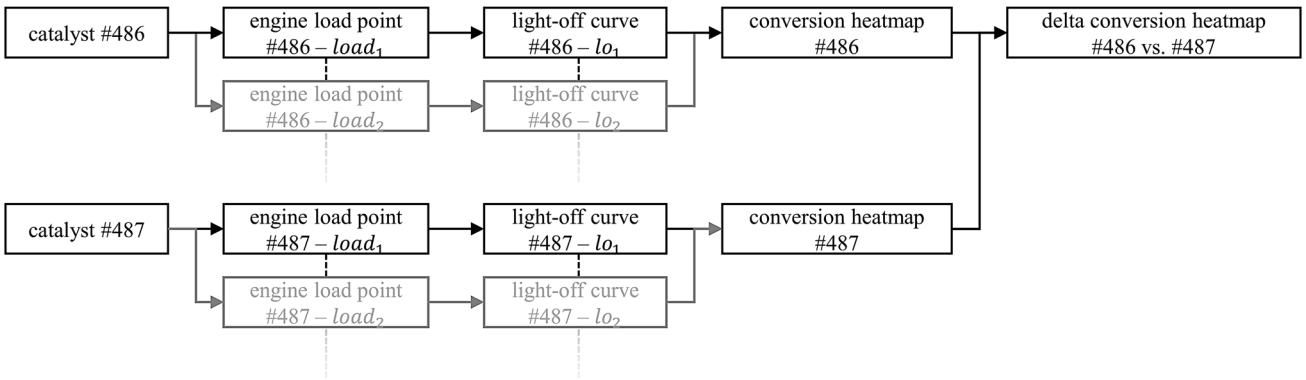

Fig. 10 Workflow for generation of a catalyst conversion heat map as well as corresponding delta maps between different catalysts

due to different aging grades and its exothermic reactions can be avoided. During each phase of constant load, the exhaust system warmed up and catalytic activity increased. After reaching a constant rate of 100%, the exhaust system was cooled down to ambient air temperature using a fuel cut overrun, supported by the electrical test bench. In this phase, the washcoat was enriched with oxygen at the end of every phase, so that identical initial start conditions for each measurement were guaranteed. The rate between raw gas and tailpipe emissions over the temperature determined the light-off curve, shown in Fig. 11 for CO emissions of exhaust system #486.

The obtained catalyst-specific light-off data served as a basis for interpolating a heat map diagram to display the conversion rate over the regulated exhaust mass flow and rising catalyst temperature area. With this compact conversion performance illustration, detailed performance comparisons of differently aged catalysts or different types of exhaust systems can be provided. Figure 12 gives an example of two conversion and a resulting calculated delta conversion heat map, illustrating the performance differences for NO_x emissions after aging of the systems.

During the presented experimental study, the delta conversion heat map proved to display the aging intensity of different catalysts in an easy and fast way. Areas with significant performance differences depending on exhaust temperature and mass flow can be easily identified. The delta conversion heat map, shown in Fig. 12, exhibits performance differences close to 50 percent between 300 and 400 °C exhaust temperature for a mass flow over 100 to 400 kg per hour.

4 Results and discussion

4.1 Influence on oxygen storage capacity

Triggered lean to rich switches were used for determination of OSC of the three-way catalysts, as explained in chapter 8.3. The OSC values of all catalysts exhibited comparable levels before aging as expected. Due to different aging processes, only small reductions were identified, which do not allow for a differentiation regarding the aging intensity based on the AFR frequency and amplitude variation. Therefore, the further evaluation focused on differences in light-off behavior and the corresponding conversion maps.

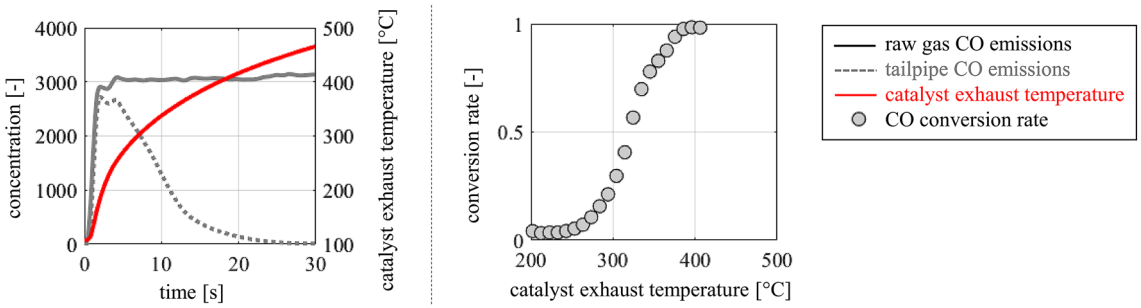

Fig. 11 Measurement and calculation of load specific CO-light-off curve of exhaust system #486

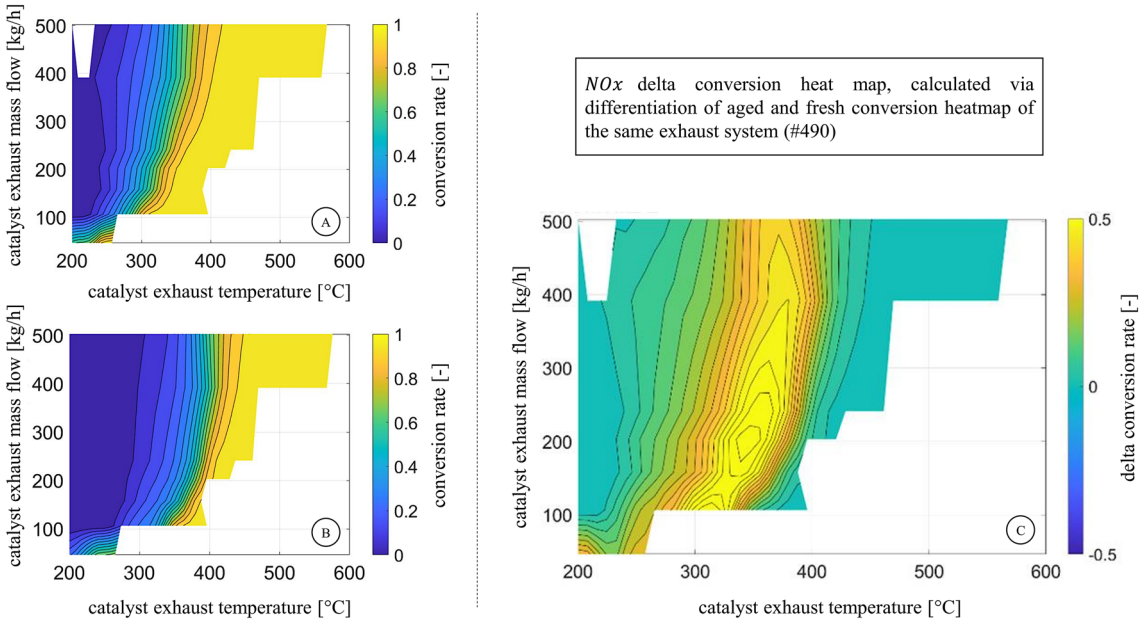

Fig. 12 interpolated conversion heat map of exhaust system #490 before (**A**) and after (**B**) aging process, as well as the calculated delta conversion heat map (**C**) with positive values representing for reduced conversion, resulting by subtraction **B** from **A**

4.2 Influence on light-off behavior and conversion efficacy heat maps

After conditioning, all exhaust systems displayed a comparable light-off behavior. No significant performance differences were documented on fresh systems. After performing the aging processes, parts could be assigned to different groups. The exhaust system aged without an AFR swing showed a small shift of the light-off curve to higher temperature only, whereas a more intense negative shift was observed for systems aged with an AFR swing. Besides the shift, the curves of systems aged with an AFR swing were also stretched compared to the one without swing and the 100% conversion rate is reached at higher temperatures only. Indications are that enlargement of the AFR amplitude seems to exhibit the most profound impact on the catalyst aging within this experimental series. The described shift in light-off behavior is presented in Fig. 13 displaying the NO_x light of curve of all four aged catalyst exhaust systems.

The deviations caused by variation of frequency and amplitude within this experiment cannot be clearly identified directly by comparison of light-off curves, but can be clearly displayed by use of conversion heat maps. The performance differences between the fresh and aged condition of catalyst numbers #487 (normal AFR), #488 (low AFR frequency) and #499 (high AFR amplitude) are provided in Fig. 14. By comparing the delta heat maps regarding the area between 300 and 400 °C as well as for 100–400 kg/h, the performance reduction caused the aging is increasing at higher AFR amplitude as well as at higher frequency. On closer inspection, the high AFR amplitude seems to have the most intense aging effect regarding the performance loss, illustrated by a wider area with a performance reduction close to 0.5 ≙ 50%.

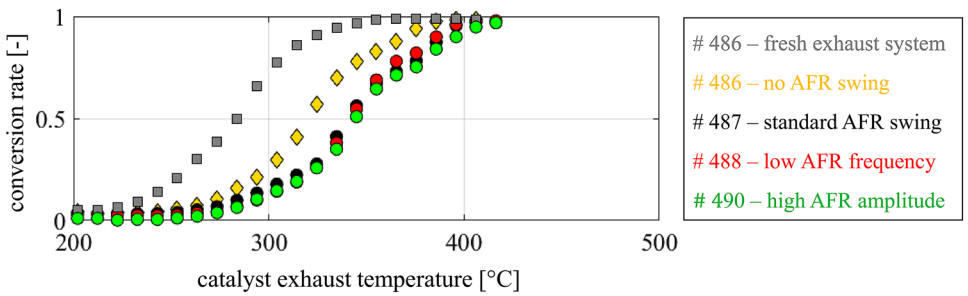

Fig. 13 NO_x light-off shift by different AFR aging variations at constant exhaust mass flow of 245 kg/h, measured over 30 s; exhaust system ID's are listed in Table 3

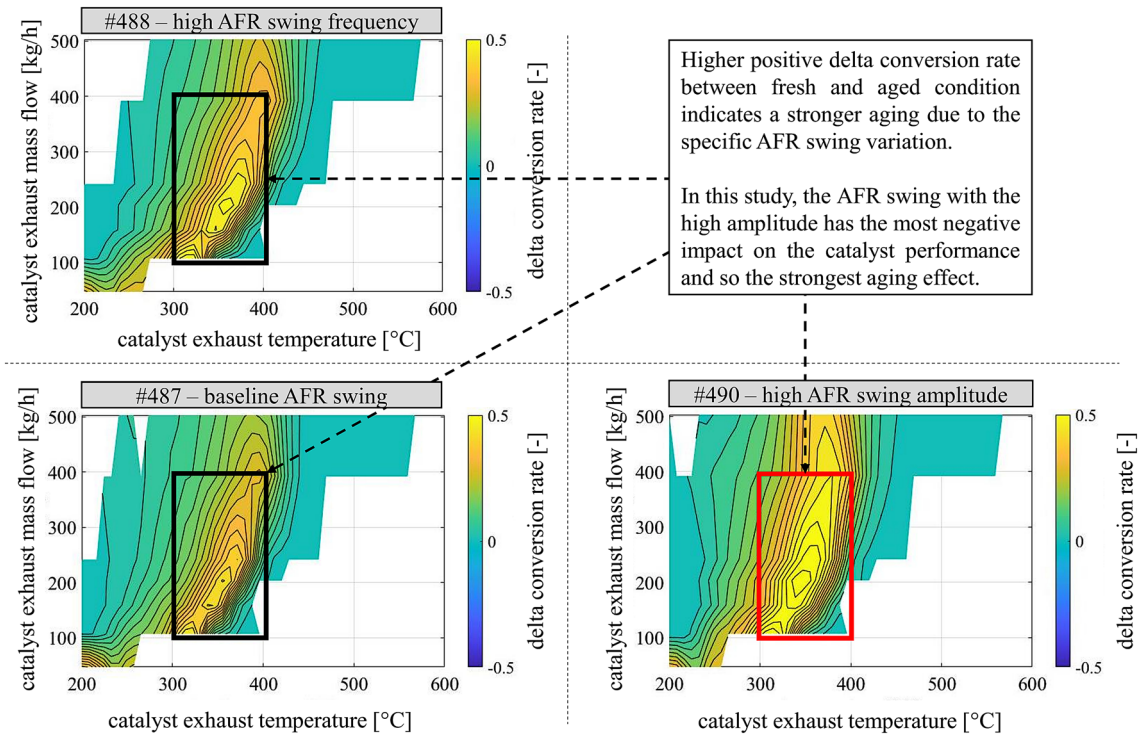

Fig. 14 NO_x delta conversion heat maps, showing aging delta between fresh and aged exhaust systems with different AFR swings over exhaust mass flow and temperature

4.3 Influence on catalyst exhaust temperature and its exothermic behavior

As described before, the aging temperature of 950 °C was determined by a 1.5 mm thermocouple, installed within the TWC (pos_1). The catalyst temperature responded to the AFR swing variation in different ways. The implementation of the AFR swing led to a temperature swing within the catalyst itself (Fig. 8—#486 vs. #487). Figure 15 displays the temperature profile of each aging cycle, measured with thermocouples placed at different positions of the exhaust system. The characteristics of the temperature oscillation within the TWC were modified via the AFR swing frequency. Increasing AFR swing period led to an increase of the temperature amplitude (#487). This behavior is the consequence of the oxygen storage and discharge due to non-stoichiometric AFR. Rich exhaust environment led to cooling due to a hydrocarbon saturation within the washcoat layer. By changing to a lean exhaust condition, excessive oxygen was employed to oxidize hydrocarbons stored on the washcoat and layer. This exothermic reaction resulted in temperature increase. Corresponding to the periodic length of the AFR swing, exhaust temperature was increased or was reduced depending on the intensity of the exothermic reaction on the catalyst surface.

While resulting in comparable temperatures of around 950 °C at pos_1, a greater AFR swing amplitude led to a bigger heat release by exothermic reaction over the catalyst length, visible by higher temperature levels after both monoliths (pos_2 and pos_3) participating in catalytic reaction (#490). Faster switches with a resulting higher amount of alternating hydrocarbons and oxygen loads intensified the conversion processes and the resulting heat release by exothermic reactions.

Figure 15 illustrates the temperature levels over the exhaust system length and the increase of the exothermic heat release by different AFR swing modes. Even though the resulting temperature rises only in a magnitude of up to 30 °C, the effect on sintering must not be underestimated. The relation of damaging sintering to temperature is exponential and can be estimated by the Arrhenius equation, described in the following chapter.

4.4 Estimation of aging effects by Arrhenius equation

The Arrhenius equation describes the dependency of temperature and reaction time. It is a commonly used method for calculating catalyst-aging times corresponding to an exhaust temperature profile of a combustion engine powered vehicle.

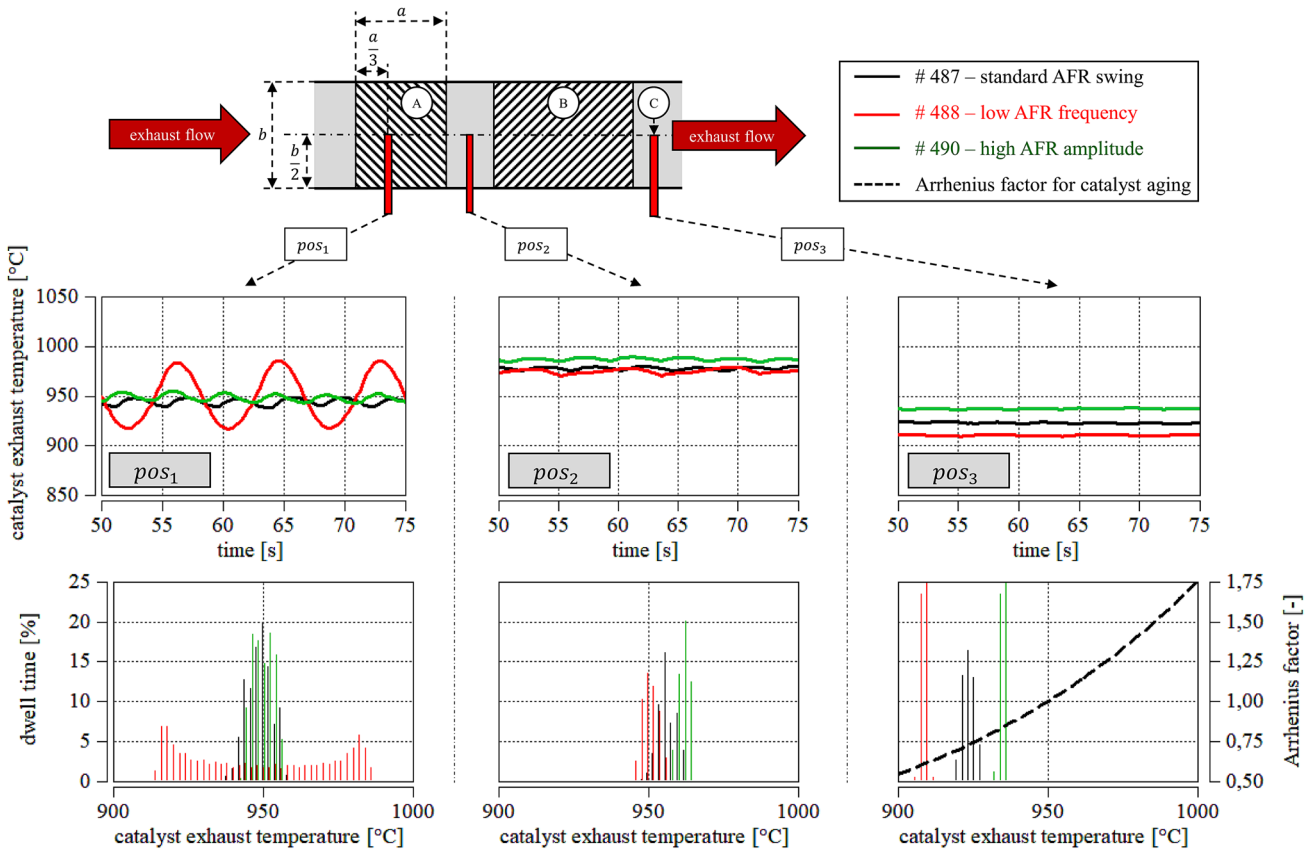

Fig. 15 Exhaust temperature trend within the exhaust system during each aging test with AFR variation and example of the Arrhenius factor for catalyst aging; **A** TWC; **B** cGPF; **C** temperature sensor (pos_1 = mid of TWC; pos_1 = downstream TWC; pos_1 = downstream GPF)

This equation was adopted by the EPA and the European legislation [20, 24, 25]. It is employed to define the catalyst thermal load on an engine test bench based on catalyst temperatures during vehicle road cycles, like the defined standard road cycle (SRC). This method allows to obtain the same catalyst thermal aging or sintering effect on an engine test bench in shorter time frames by using higher exhaust temperatures in comparison to a vehicle catalyst driven over a long time or distance. Within this experimental study, this method is used for estimating the effects of catalyst thermal aging generated by a different AFR swing.

High temperature gradients over a short time result in a higher sintering effect than lower temperature slopes over a long time. This exponential dependency is described by the following Arrhenius equation:

$$\text{Arrhenius}_{\text{factor}} = e^{\left[R\left(\frac{1}{T_r}-\frac{1}{T_v}\right)\right]} \quad \text{Arrhenius equation,} \tag{10}$$

$$t_e = t_h \times \text{Arrhenius}_{\text{factor}} \quad \text{Equivalent aging time in each temperature - bin,} \tag{12}$$

$$S_{\text{Arrhenius}} = \sum t_e \quad \text{Summation of aging time over all temperature bin.} \tag{13}$$

The temperature signals were recorded by use of several thermocouples and are displayed as time-at-temperature, shown as a histogram in Fig. 15 (50 h, shown in percentage).

T_r is the effective reference temperature. It is defined as the arithmetical mean temperature during each aging process (950 °C ≙ 1123.15 K). The mid-point value of each temperature bin is set up as T_v, with smaller bars indicating more precise results. However, setting up the bins at a value of 2 Kelvin, the calculation results are sufficient to identify sintering differences, provoked by different AFR swing characteristics. R stands for the thermal reactivity constant and is proposed to be 17,500 as a catalyst type specific deactivation

$$T_r = \frac{\int_0^{t_{\text{end}}} T_{\text{AgingCycle}}(t)\mathrm{d}t}{t_{\text{end}}} \quad \text{Effective reference temp. (950 °C} \triangleq \text{1123.15 K),} \tag{11}$$

Table 4 Sintering difference by Arrhenius equation

Test	Exhaust system ID	Normalized aging difference calculated via Arrhenius equation ($S_{Arrhenius}$) (% value of #487)					
		pos_1		pos_2		pos_3	
#2	#487	100.0		100.0		100.0	
#3	#488	102.4	≙ + 2.4	93.6	≙ − 6.4	83.0	≙ − 17.0
#4	#490	100.8	≙ + 0.8	105.9	≙ + 5.9	114.0	≙ + 14.0

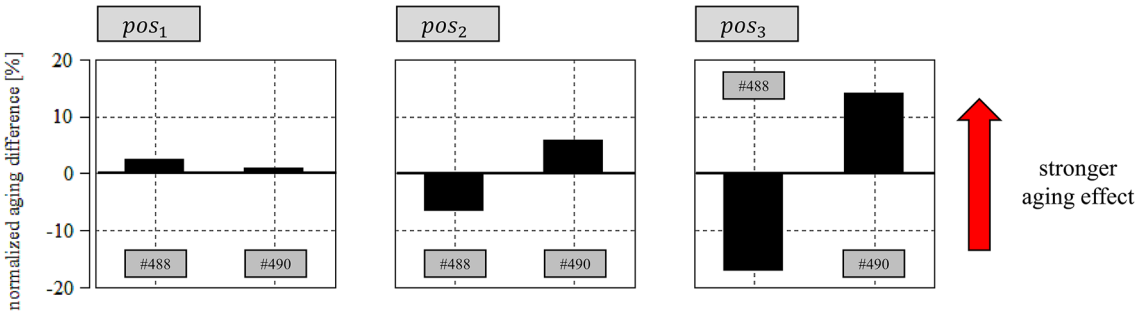

Fig. 16 Aging difference calculated via Arrhenius equation between catalysts aged with high AFR swing frequency (#488) and amplitude (#490), normalized on results from catalyst #487

time constant for exhaust aftertreatment systems according LEVIII legislation. t_h indicates the time of aging within the specific temperature bin T_v. t_e is the product of t_h and the $Arrhenius_{factor}$, whereas its summation represents the overall time of required aging.

During this analysis, t_e was calculated for all temperature sensors of each catalyst aging experiment. Afterwards, the results of each temperature sensor were normalized on the exhaust system #487 to show aging differences by the Arrhenius quotation in percentages caused be different exhaust temperatures, listed in Table 4 and illustrated in Fig. 16.

According to the results, the front area of the catalyst is affected most intensely by a low AFR frequency (#488) and high temperature amplitudes. By comparing the values downstream of the TWC and the cGPF, the effect turns opposite. The sintering effect declines over the length of the catalytic system and the sintering induced by a high AFR amplitude becomes dominant (#490). The total degradation of the exhaust system is calculated to be mostly pronounced by extending the AFR amplitude according to the Arrhenius equation. However, as most of the chemical reactions take part in the front surface of the catalyst, sintering this part must not be underrated as seen by comparison of the conversion maps #487 and #488 (Fig. 14).

5 Conclusion and outlook

The effect of an AFR swing and its variation in terms of amplitude and frequency on catalyst aging was investigated on a turbo-charged eight-cylinder engine. To guarantee the thermic durability of the turbocharger, the T3 temperature was reduced by using a rich AFR swing around 0.85 combined with a constant secondary air injection within the exhaust path. An additional mixer was set up upstream of the catalyst to ensure a homogeneous exhaust gas mixture.

The increased catalyst aging due to an AFR swing was clearly demonstrated as well as the possible effects of swing variation regarding frequency and amplitude. By expanding the time of oscillation, the amplitude of the temperature swing, induced by the AFR swing, increased in the middle of the catalyst. Due to the exothermic reaction, the temperature increased with the catalyst's length. By expanding the AFR amplitude, the temperature swing within the catalyst was not as distinctive as at the lower AFR frequency, but the temperature level behind the monoliths was strongly elevated. This reaction led to a higher exothermic reaction in the catalyst and a probably higher sintering, corresponding to a more intense aging behavior.

Under consideration of the Arrhenius equation, different light-off results can be explained. Due to more intense

exothermic reactions, different magnitudes of sintering effects have been observed. To reduce the aging effect of the AFR swing on the catalyst exhaust system to a possible minimum, the overall AFR swing has to be minimized. A reduction of the frequency reduces the sintering of the TWC front surface, whereas a small amplitude decreases the exothermic reaction with lower temperatures over the catalyst's length.

This effect can also be analyzed in detail by examining the monoliths with additional physical and chemical analysis methods. Physisorption and chemisorption will be used for analyzing the surface as well as the sorption behavior in different areas within the monoliths. To receive a better differentiation regarding the results of the experiments, the aging time of 50 h will be prolonged. In addition to this, a synthetic hot-gas test bench can increase the resolution of the light-off curve by controlling the exhaust temperature and mass flow more precisely. A reduction of the temperature sensor inertia by reducing the diameter can have a positive influence on the measurement resolution as well.

Acknowledgements This work was supported by the IFKM (Institut für Kolbenmaschinen) at Karlsruhe Institute of Technology (KIT) and financially supported by the Mercedes-AMG GmbH.

Author contributions René Eickenhorst wrote the whole manuscript text and prepared all figures. All authors, René Eickenhorst and Prof. Dr. sc. techn. Koch, reviewed the manuscript.

Funding Open Access funding enabled and organized by Projekt DEAL.

Declarations

Conflict of interest On behalf of all authors, the corresponding author states that there is no conflict of interest.

References

1. Europäischen Union (EU): Zur Ergänzung der Verordnung (EG) Nr. 715/2007 des Europäischen Parlaments und des Rates über die Typgenehmigung von Kraftfahrzeugen hinsichtlich der Emissionen von leichten Personenkraftwagen und Nutzfahrzeugen (Euro 5 und Euro 6), EU Verordnung 2017/1151 (2017)
2. European Union (EU): Regulation (EC) No 715/2007 of the European Parliament and of the Council of 20 June 2007 on type approval of motor vehicles with respect to emissions from light passenger and commercial vehicles (Euro 5 and Euro 6) and on access to vehicle repair and maintenance information (Text with EEA relevance), Regulation Number: 715/2007 (EC) (Euro 5/ Euro 6) (2018/858) (2018)
3. European Commission: Proposal for a regulation of the European Parliament and the Council on type-approval of motor vehicles and engines and of systems, components and separate technical units intended for such vehicles, with respect to their emissions and battery durability (Euro 7) and repealing Regulations (EC) No 715/2007 and (EC) No 595/2009, COM(2022) 586 final ANNEXES 1 to 6 (2022)
4. Riegel, J., Neumann, H., Wiedenmann, H.-M.: Exhaust gas sensors for automotive emission control. Solid State Ionics. Elsevier (2002)
5. Louen, C.J.: Datenbasierte Zustandsüberwachung in Personenkraftwaren mit Anwendung an einem Drei-Wege-Katalysator. Springer (2016)
6. Feßler, D.K.: Modellbasierte On-Board-Diagnoseverfahren für Drei-Wege-Katalysatoren. Instituts für Regelungs- und Steuerungssysteme, Karlsruher Institut für Technologie (2010)
7. Lassi, U.: Deactivation correlations of PD/RH three-way catalysts designed for EURO IV emission limits. Department of Process and Environmental Engineering, University of Oulu (2003)
8. Hagelücken, C., Tilgner, I.-C.: Autoabgaskatalysatoren, expert Verlag (2016)
9. Zheng, T., Lu, B., Harle, G., Yang, D., Wang, C., Zhao, Y.: A comperative study on Rh-only, Pd-only and Pd/Rh catalysts. Applied catalysis A, general. Elsevier (2020)
10. Odendall, B.: Ein vereinfachtes Modell des Lambda-geregelten Dreiwegekatalysators zum Einsatz in Motor-Steuergeräten zur On-Board-Diagnose. Energie-, Verfahrens- und Biotechnik der Universität Stuttgart, Universität Stuttgart (2003)
11. Koltsakis, G.C., Stamatelos, A.M.: Catalytic automotive exhaust aftertreatment. Prog. Energy Combust. Sci. **23** (1997)
12. Sabertec, L.L.C.: Three-way catalysts: aging, causes of failure and deactivation (2022). https://www.ecooptimized.com/index.php/gasoline/80-three-way-catalysts-aging-causes-of-failure-and-deactivation-.html. Accessed on 28th Nov 2022
13. Beck, D.D., Sommers, J.W., DiMaggio, C.L.: Impact of sulfur on model palladium-only catalysts under simulated three-way operation, applied catalysis environmental. Elsevier Science B V (1993)
14. Taha, R., Duprez, D., Mouaddib-Moral, N., Gauthier, C.: Oxygen storage capacity of three-way catalysts: a global test for catalyst deactivation. Catalysis and automotive pollution control IV. Elsevier Science B.V. (1998)
15. Winkelhofer, E., Hirsch, A., Philipp, H., Trifterer, M., Berglez, M.: Powertrain calibration techniques, SAE International (SAE 2019-24-0196) (2019)
16. Gong, C., Huang, K., Deng, B., Liu, X.: Catalyst light-off behavior of a spark-ignition LPG (liquefied petroleum gas) engine during cold start, energy. Elsevier (2011)
17. Samimi, O., Abdolmaleki, S., Rudaki, J.: Comparison of aged and fresh automotive three-way catalysts in real driving. In: Sixth International Conference on Internal Combustion Engines (2009)
18. Brisley, R.J., O'Sullivan, R.D., Wilkins, A.J.J.: The effect of high temperature ageing on Platinum–Rhodium and

Palladium–Rhodium three way catalysts. International Congress & Exposition, SAE Technical Paper (1991)
19. Flynn, P.C., Wanke, S.E., Turner, P.S.: The limitation of the transmission electron microscope for characterization of supported metal catalysts. J. Catal. **33** (1973)
20. Galassi, M.C., Martini, G.: Durability demonstration procedures of emission controll devices für Euro 6 vehicles, JRC Science and policy reports. Publications Office of the European Union (2014)
21. Sideris, M.: Methods for monitoring and diagnosing the efficiency of catalytic converters, vol. 115. Studies in surface science and catalysis. Elsevier (1998)
22. Descorme, C., Taha, R., Mouaddib-Moral, N., Duprez, D.: Oxygen storage capacity measurement of three-way catalysts under transient conditions, applied catalysis A. Elsevier (2022)
23. Cybulski, A., Moulijn, J.A.: Monoliths in heterogeneous catalysis. Catal. Rev. Sci. Eng. (1994)
24. EPA (Environmental Protection Agency): Emission durability procedures and component durability procedures for new light-duty vehicles, light-duty trucks and heavy-duty vehicles; final rule and proposed rule, EPA—Federal Register, vol. 71, no. 10, 40 CFR Part 86 (2006)
25. Ignatov, D., Küpper, C., Pischinger, S., Bahn, M., Betton, W., Rütten, O., Weinowski, R.: Catalyst aging method for future emissions standard requirements. SAE International (2010)